Organo-LDH synthesized via tricalcium aluminate hydration in the presence of Na-dodecylbenzenesulfate aqueous solution and subsequent investigation by Near-infrared and Mid-infrared spectroscopy

Ping Zhang [a,b,c], Tianqi Wang [a], Guangren Qian[b*], Ray L. Frost[c**]

[a] *Key Laboratory of Poyang Lake Environment and Resource Utilization, Ministry of Education, School of Environmental and Chemical Engineering, Nanchang University, Nanchang 330047, China;*

[b] *School of Environmental and Chemical Engineering, Shanghai University, Shanghai 200072, PR China.*

[c] School of Chemistry, Physics and Mechanical Engineering, Science and Engineering Faculty, Queensland University of Technology, GPO Box 2434, Brisbane Queensland 4001, Australia.

Corresponding Authors:

Ray L. Frost: Tel: +61-7-3138 2407;

Fax: +61-7-3138 2407

Email: r.frost@qut.edu.au

Guangren Qian: Tel: +86-13699508783;

Fax: +86-791-82087843

E-mail: zhangping@ncu.edu.cn

Abstract: Na-dodecylbenzenesulfate (SDBS), a natural anionic surfactant, has been successfully intercalated into a Ca based LDH host structure during tricalcium aluminate hydration in the presence of SDBS aqueous solution (CaAl-SDBS-LDH). The resulting product was characterized by powder X-ray diffraction (XRD), mid-infrared (MIR) spectroscopy combined with near-infrared (NIR) spectroscopy technique, thermal analysis (TG-DTA) and scan electron microscopy (SEM). The XRD results revealed that the interlayer distance of resultant product was expanded to 30.46 Å. MIR combined with NIR spectra offered an effective method to illustrate this intercalation. The NIR spectra (6000 - 5500 cm^{-1}) displayed prominent bands to expound SDBS intercalated into hydration product of C_3A. And the bands around 8300 cm^{-1} were assigned to the second overtone of the first fundamental of C-H stretching vibrations of SDBS. In addition, thermal analysis showed that dehydration and dehydroxylation took place at ca. 220 ^oC and 348 ^oC, respectively. And SEM results appeared approximately hexagonal platy crystallites morphology for CaAl-SDBS-LDH, with particle size smaller and thinner.

Keywords Tricalcium aluminate (C_3A); Sodium dodecyl benzene sulfonate (SDBS); Intercalation； Near-infrared (NIR); Middle-infrared (MIR) spectroscopy;

1. Introduction

Layered double hydroxides (LDHs), also called anionic clays, are normally composed of positively charged metal oxides /hydroxide layers and exchangeable interlayer inorganic anions, organic anionic, poly (acrylic acid) and superplasticizers [1, 2]. The general chemical formula for LDHs are expressed of $[M_{1-x}^{II} M_x^{III}(OH)_2]^{x+}[A_{x/n}^{n-}]\cdot yH_2O$, where M^{II} and M^{III} represent metal cations and A^{n-} the interlayer anions [3]. LDHs have one of outstanding property that a variety of anionic species, specially organic anions, can be inserted by guests into the interlayer region assembling organic-LDH, of which the intrinsic hydrophilic surface property can be changed into hydrophobic one [4, 5]. Modified LDHs with larger surfactant anions lead to larger interlayer region for increasing adsorption capacity. Recently, the hydrophobic nature and accessibility of the interlayer region of organo-LDHs increase their materials adsorption species, such organic pollutants of non-polarity or low polarity in the environment [6-8].

Hydration of tricalcium aluminate (C_3A), which is an influent constituent in cement produces layered double hydroxides, namely $2CaO \cdot Al_2O_3 \cdot 8H_2O$ (C_2AH_8) and $4CaO \cdot Al_2O_3 \cdot 13H_2O$ (C_4AH_{13}). Their structures reveal $[Ca_2Al(OH)_6^{+}]$ main layers with OH^- anions and H_2O molecules in the interlayer region [9, 10]. It is easier to trap other anions such as Cl^-, SO_4^{2-} $CO_3^{2-}$to form hydrocalumite. Typically, one of hydrocalumite with chloride is the major and stable hydration of C_3A in cement paste/concrete subjected to sea water attack [11]. So as hydration of C_3A can be easily and cheaply combined with anions to form to Ca based LDHs. In our previous research, we focus on introducing Na-dodecylsulfate (SDS) of

Na-dodecylbenzenesulfate (SDBS) into resulting products from hydrocalumite [12, 13]. In fact, it have been reported that comb-shaped polycarboxylates which are used as superplasticizers in concrete can also introduce into the hydration of C_3A interlayer region [14]. Generally, the structure of most LDHs intercalated by guest anions is via to X-ray diffraction (XRD), mid-infrared (MIR) spectroscopic methods [15, 16]. In addition, near-infrared (NIR) has been widely application in clay mineral such as organoclays, kaolinite group minerals and montmorillonite [17, 18]. This technique can be useful to measure overtones and combination bands of the fundamental vibration of O-H, N-H and C-H bands in the mid-infrared region [19, 20]. Therefore, combined with MIR spectroscopy and NIR spectroscopy have been supported as an alternative analytical method as they are fast, convenient and nondestructive [21]. However, there are few reports on using this combination technique to verify modified LDHs.

In the present study, this research focuses on using C_3A directly to adsorb SDBS from aqueous media. The objectives of this research are to (1) investigate the structure and morphology of resulting product for SDBS adsorbed with C_3A; and (2) combined with MIR and NIR spectroscopy to evaluate the SDBS intercalation into the interlayer of hydration of C_3A, which demonstrate that the NIR region provide information comparable with that obtained by MIR and afford effective method to illustrate the SDBS is intercalated into direct hydration of C_3A successfully.

2. Experimental and methods

2.1. *Materials preparation*

The organo-LDH phase, named as CaAl-SDBS-LDH, was prepared by the hydration of C_3A with 0.2 mol/L SDBS solution. Firstly C_3A was synthesized through the solid phase reaction. In brief, reagent grade $CaCO_3$ and low-alkali Al_2O_3 at a molar ratio of 3:1 were heated at 1300–1350 °C. The heating process was conducted in quartz crucibles and continued until X-ray powder diffraction and a modified Franke test showed that the free lime content was reduced to below

0.5%. Then 50 ml of SDBS solution with 0.2 M SDBS was mixed with as-prepared C_3A and shaken at 150 rpm in a thermostatic bath shaker at 25 ± 1 °C. After stirring, the mixture was aged at 60-70 °C for a further 24 h. The slurry was washed with distilled water, and dried at 70 °C overnight. Then the dried sample was ground, passed through 100 mesh sieve and stored in a desiccator for further use.

2.2. *X-ray diffraction*

Powder X-ray diffraction (XRD) patterns were collected using a D/max RBX diffractometer, using Cu-K_α (40 kV, 100mA) radiation at 6° min^{-1} between 5.0°and 65° 2θ angles. In particular, these samples were carefully scanned in 2θ=2-15° at a scanning rate of 2° per minute using silts 1/6 (divergence), 1/6 (anti-scattering) and 0.15 (receiving). All samples were prepared for X-ray diffraction as a random pressed powder.

2.3. *Mid-infrared spectroscopy*

The Mid-infrared spectra were obtained using the Thermo Nicolet AVATAR 370 Fourier transform infrared (FT-IR) spectrometer with a smart endurance single bounce diamond ATR cell. 64 scans were co-added for each measurement over the spectral range of 4000-400 cm^{-1} with a resolution of 4 cm^{-1}.

Near-infrared spectra were collected in reflectance mode using a Nicolet Nexus FT-IR spectrometer with a Nicolet Near-IR Fibreport accessory (Nicolet Nexus, Madison, Wisconsin, USA). A white light source was used, with a quartz beam splitter and TEC NIR In Ga As detector. Spectra were obtained from 12,000 to 4000 cm^{-1} (909-2500 nm) by the co-addition of 64 scans at a resolution of 8 cm^{-1}. A mirror velocity of 1.2659 m/s was used.

The spectral manipulations of baseline adjustment, smoothing, and normalization were performed using the Spectracalc software package GRAMS (Galactic Industries Corporation, NH, USA). Band component analysis was carried out using Peakfit software (Jandel Scientific, Postfach 4107, D-40688

Erkrath, Germany). Lorentz-Gauss cross product functions were used throughout, and peakfit analysis undertaken until squared correlation coefficients with $r^2 > 0.998$ was obtained.

2.4 *SEM*

The morphology of the resulting products was examined with scanning electron microscopy (SEM) with an S-2360 microscope (Hitachi). Before loading, the samples were ultrasonically dispersed in ethanol solution.

3. Results and discussion

3.1. *XRD analysis*

The XRD patterns of the reaction products between C_3A and C_3A modified by SDBS as well as product of hydrated C_3A (C_4AH_{19}) as reference are shown in Fig.1. The first basic reflection corresponding to the highest *d*-value gives information about the interlayer distance. As shown in Fig.1(a), a strong first reflection of C_4AH_{19} located in 8.18 ^{o} (2θ) was displayed obviously that a basal *d*-value was 10.6 Å. After C_3A was added into 0.2M SDBS aqueous solution, the reflection of the collected solid corresponding to (002), (004), (006) crystal planes were recorded at low angles, such as 2.91^o, 5.86^o, and 9.04^o, and their corresponding distances of spacing were depicted multiple relationship, indicating obviously well-formed double layered structure, with the basal spacing $d_{(002)}$ was 30.46 Å, which are expanded to 19.86 Å compared with C_4AH_{19}. Owing to the increase of the basal spacing of the layered materials, the diffraction peak represented the interlayer spacing shift to a lower 2θ value [22]. The results were very powerful to illustrate that SDBS anion was intercalated into interlayer of CaAl-LDH during hydration of C_3A occurring and formed new LDH phase. Based on researches earlier reported that a thickness of 4.8 Å for CaAl-LDH main layer [23], the interlayer spacing was calculated to be 19.86 Å. In theory, the length of SDBS anion is 21 Å [24], an interlayer spacing of 17.8 Å and 35.6 Å would be shown for monolayer and bilayer models with perpendicular orientation of the Na-dodecylsulfate in the interlayer, respectively [13]. Thus, the interlayer spacing of CaAl-SDBS-LDH is between that of monolayer and bilayer in our research, so it can

be deduced that its conformation of SDBS ion in interlayer was a inter-penetration bilayer model. Moreover, it was revealed obviously in Fig.1(b) that some peaks of C_3A (marked with *) were still existed in XRD pattern of CaAl-SDBS-LDH, suggesting that intercalation did not finish completely between DBS^- ion and C_3A. It was possible due that the hydration process taking place the surface of C_3A to restraint SDBS combined with C_4AH_{19} to form LDH.

3.2 ***Mid-infrared spectroscopy***

The mid-infrared spectra of C_3A and C_3A modified by SDBS in 4000-500 cm^{-1} are displayed in Fig.2 and the results reported in Table 1. There is obvious difference between the MIR spectra of C_3A and CaAl-SDBS-LDH in the range of 4000-500 cm^{-1}. In the case of C_3A, there were only obviously shown the bands in the range of 900-500 cm^{-1} mainly attributed to M-O lattice vibrations (M-OH, M-O-M or O-M-O), with no bands observed in 4000-900 cm^{-1}. It was perfectly suitable for the structure of C_3A, which was only assemble by calcium oxide (Ca-O) and aluminium oxide (Al-O). In contrast, the MIR spectra of CaAl-SDBS-LDH bands were obviously located into three regions, 4000-2500 cm^{-1}, 2000-900 cm^{-1}, 800-500 cm^{-1} respectively. For 4000-2500 cm^{-1} region, the positions and relative intensities of the bands due to typical C-H stretch ($\nu_{as}(CH_3)$) at 2960 cm^{-1}, $\nu_{as}(CH_2)$ at 2930 cm^{-1}, and $\nu_{as}(CH_2)$ at 2851 cm^{-1}, closely resemble those found in the literature [25]. In the infrared spectrum between 3800 and 2800 cm^{-1} characteristic bands appeared in 3640, 3600 and 3475 cm^{-1} attributed to the stretching vibrations of lattice water and OH groups. Moreover, the bands in 3650, 3569 and 3400 cm^{-1} represent the stretching vibrations of interlayered water and OH groups. Compare to the IR spectra of CaAl-Cl-LDH in this region reported related literature [24], the positions of these bands shift to lower wave-numbers upon reaction with SDBS, which was suggested that the surface property of organo-LDH was changed from hydrophilic to hydrophobic [26]. For 2000-900 cm^{-1}, the bands at 1015, 1040, 1176, 1216, 1134, 1412, 1460 cm^{-1} were ascribed to C-H aromatic in-plane bend (1015 and 1134 cm^{-1}), S=O symmetric stretch and anti-symmetric stretch (1040 and 1216 cm^{-1}), the S=O anti-symmetric stretch

(1176 cm^{-1}), and C-C aromatic stretch (1412 and 1460 cm^{-1}), closely similar to those reported in the literature referred to CaAl-LDH-SDBS synthesized by SDBS intercalated into CaAl-Cl-LDH [24]. Besides, it is well known that IR spectroscopy is very sensitive to carbonate anion (1425 cm^{-1}), with the very weak band here it was assumed that the prepared sample was carbonate free. As for 800-500, there were still appeared bands represented M-O lattice vibrations, and these bands were obviously shifted to lower wave-numbers compared to C_3A, owing to the formation of hydrogen bonding of benzenesulfonate with the OH group of the layer as well as with the interlayer water via H-O-*M* besides the electrostatic attraction and the possible hydrophobic interaction between the interlayer DBS anions. Based on the above results, it was proved that SDBS was intercalated into hydration product of C_3A and formed CaAl-LDH-SDBS successfully.

3.3 ***NIR spectroscopy***

The NIR spectra are the result of energy absorption by organic molecules [19] and often named as proton spectroscopy. Besides, the NIR spectroscopic technique mainly measures overtones and combination bands of the fundamental vibration of O-H, N-H and C-H bands in the mid-infrared region [17, 19]. Usually, the near IR spectra may be conveniently divided into sections according to the attribution of bands in this spectral region. Based on C_3A used in the experiment, which only contains M-O bonds, accordingly near IR spectra of C_3A had no bands in this region. It was focused on revealing the near IR spectra of C_3A modified by SDBS. There were only broad bands in the region of 5500-4800 cm^{-1}, which attributed to the overtones of water OH vibrations. And the corresponding bands ranged from 4700 to 4000 cm^{-1} region became complex, bands at 4644, 4609, 4330, 4393, 4260 and 4180 cm^{-1} with variable band positions and diminishing intensity were observed, it was attributed to the combination of the symmetric stretching modes of the $(CO_3)^{2-}$ anion and CH groups. Besides, three bands at 5870, 5815 and 5776 cm^{-1} were displayed which corresponding to the overtones of C-H stretching vibrational modes, which were attributed the overtone bands $2\nu_{as}(CH_3)$, $2\nu_{as}(CH_2)$ and $2\nu_{s}(CH_2)$,

233 respectively. Moreover, the bands were observed for CaAl-SDBS-LDH at 7193, 7093,
234 6907 and 6859 cm^{-1} and were assigned to the first fundamental overtone of the OH
235 stretching vibrations at ca.3500 cm^{-1} in MIR spectrum for CaAl-SDBS-LDH. It was
236 also observed weaker bands around 8300 cm^{-1}, which was C-H overtone stretching
237 vibrations [19]. The above mentioned were closely similar to those reported in the
238 literature referred to LDH intercalated by SDBS [24], suggesting again combined with
239 C_3A to form LDH.

240 **3.4 *Thermal analysis***

241 The TG-DTA curves of C_3A and CaAl-SDBS-LDH are shown in Fig. 3. Compared
242 with the curve of C_3A (Fig. 3 a), three major weight loss stages of 9.98 % around 220
243 ^oC, 9.15 % around 410^oC, and 20.26 % after 578 ^oC were observed in the TG curve of
244 CaAl-SDBS-LDH, which was correspond to the loss of adsorbed lattice water
245 molecules, dehydroxylation of the layer and the decomposition of SDBS respectively.
246 In the case of the DTA curve of CaAl-SDBS-LDH, the endothermic peaks was
247 appeared at 220 ^oC, 410^oC and 578 ^oC, which were perfectly suitable for the TG curve.
248 These results indicated that CaAl-SDBS-LDH contained obviously adsorbed and
249 interlayered water, and the dehydration temperature were all lower than that of LDHs
250 which interlayer spacing composited inorganic ions, such as Cl^- [12]. It was possibly
251 resulted from the hydrophobic nature of interlayer surface enchanced to lead to
252 interlayered water adsorbing power reduced In addition, we could find that
253 CaAl-SDBS-LDH was the mass loss at ca.810 ^oC, related to an exothermic peak in
254 DTA curve, which was attributed to LDH structure collapse [27]. The total mass loss
255 was 39.4%, which was higher than that of C_3A. All thermal results could illustrate that
256 SDBS was intercalated into the hydrated of C_3A and formed organo-LDH.

257 3.5 ***Scan Electron Microscopy (SEM).***

258 The SEM micrographs of C_3A and CaAl-SDBS-LDH are shown in Fig.4.
259 Compared with C_3A, the resulting solid of CaAl-SDBS-LDH appeared obvious
260 changes in morphology, which the approximately hexagonal platy crystallites were
261 observed in overall morphology. And the particle plates changed to a layered structure,

which was just identical with the XRD results. Moreover, the particle size of CaAl-SDBS-LDH changed to smaller and thinner, which was accord with some references related to organo-LDHs [13]. It was due to the aggregation of crystal particle. restrained effectively by SDBS.

4. **Conclusions**

Novel organo-LDH nanohybrids were successfully synthesized by hydration of C_3A in the presence of SDBS aqueous solution, which was illustrated by the combination of the MIR and NIR spectroscopic methods complemented with XRD, TG-DTA and SEM analysis. This research expounded that SDBS could be intercalated into interlayer spacing during C_3A occurring hydration reaction and formed organo-LDH, with the interlayer distance was 30.46 Å. MIR combined with NIR spectra offered an effective method to assist evidence for this intercalation. The regions from 6000 to 5500 cm^{-1} are more obvious to examine SDBS intercalated into hydration product of C_3A. In addition, it is also revealed that the bands around 8300 cm^{-1} are assigned to the second overtone of the first fundamental of C-H stretching vibrations of SDBS.

Acknowledgments

The authors gratefully acknowledge infrastructure and morphology checking support of the Queensland University of Technology, Chemistry Discipline, Faculty of Science and Technology. This project is financially supported by Postdoctoral Science Foundation of China No. 2012M511456 and Postdoctoral Science Foundation of Jiang xi Province No.13006440.

References

1. Ma, X., et al., Hydrothermal preparation and anion exchange of Co2+-Ni2+-Fe3+ CO32- LDHs materials with well regular shape. Journal of Colloids and Surfaces A: Physicochemical and Engineering Aspects,. 371(2010) 71-75.
2. Wang, H., et al., Facile Sodium Alginate Assisted Assembly of Ni−Al Layered

290 Double Hydroxide Nanostructures. Industrial & Engineering Chemistry Research, 49
291 (2010) 2759-2767.
292 3. Bellezza, F., et al., Synthesis of colloidal dispersions of NiAl, ZnAl, NiCr, ZnCr,
293 NiFe, and MgFe hydrotalcite-like nanoparticles. Journal of Colloid and Interface
294 Science,. 376 (2012) 20-27.
295 4. Xiong, Z. and Y. Xu, Immobilization of Palladium Phthalocyaninesulfonate onto
296 Anionic Clay for Sorption and Oxidation of 2, 4, 6-Trichlorophenol under Visible
297 Light Irradiation. Chem. Mater,. 19 (2007): 1452-1458.
298 5. Legrouri, A., et al., Removal of the herbicide 2, 4-dichlorophenoxyacetate from
299 water to zinc¨Caluminium¨Cchloride layered double hydroxides. Water Research, 39
300 (2005) 3441-3448.
301 6. Bruna, F., et al., Organo/LDH nanocomposite as an adsorbent of polycyclic
302 aromatic hydrocarbons in water and soil–water systems. Journal of Hazardous
303 Materials, 225–226 (2012.) 74-80.
304 7. Yang, Y., et al., Adsorption of perchlorate from aqueous solution by the
305 calcination product of Mg/(Al–Fe) hydrotalcite-like compounds. Journal of Hazardous
306 Materials, 209–210 (2012) 318-325.
307 8. Shi, Z., et al., Photolysis of 2-chlorophenol dissolved in surfactant solutions.
308 Environ. Sci. Technol,. 31(1997) 3581-3587.
309 9. Wu, Y., et al., Effective removal of selenate from aqueous solutions by the Friedel
310 phase. Journal of Hazardous Materials, 176(2010) 193-198.
311 10. Yu, B., H. Bian, and J. Plank, Self-assembly and characterization of Ca-Al-LDH
312 nanohybrids containing casein proteins as guest anions. Journal of Physics and
313 Chemistry of Solids, 71 (2010.) 468-472.
314 11. Bothe, J. and P. Brown, PhreeqC modeling of Friedel's salt equilibria at 23¡À1¡ã
315 C. Cement and Concrete Research, 34 (2004) 1057-1063.
316 12. Zhang, P., et al., Na-dodecylsulfate modification of hydrocalumite and subsequent
317 effect on the structure and thermal decomposition. Journal of Thermal Analysis and
318 Calorimetry, 104 (2010) 1-5.

13. Ping Zhang, G.Q., Zhi Ping Xu, Huisheng Shi, Xiuxiu Ruan Jing Yang, Ray L. Frost, Effective adsorption of sodium dodecylsulfate (SDS) by hydrocalumite (CaAl-LDH-Cl) induced by self-dissolution and re-precipitation mechanism. Journal of Colloid and Interface Science,. 367 (2012) 7-14.

14. Cheng, M.-Y. and B.-J. Hwang, Control of uniform nanostructured [alpha]-Ni(OH)2 with self-assembly sodium dodecyl sulfate templates. Journal of colloid and interface science, 2009. 337(1): p. 265-271.

15. Cai, P., et al., Competitive adsorption characteristics of fluoride and phosphate on calcined Mg–Al–CO3 layered double hydroxides. Journal of Hazardous Materials, 213–214 (2012) 100-108.

16. Lv, T., et al., Physicochemical characterization and sorption behavior of Mg–Ca–Al (NO3) hydrotalcite-like compounds toward removal of fluoride from protein solutions. Journal of Hazardous Materials, 24 (2012) 234-242

17. Cheng, H., et al., A spectroscopic comparison of selected Chinese kaolinite, coal bearing kaolinite and halloysite--A mid-infrared and near-infrared study. Spectrochimica Acta Part A: Molecular and Biomolecular Spectroscopy, 77(2010) 856-861.

18. Chung, H., M.-S. Ku, and J.-S. Lee, Comparison of near-infrared and mid-infrared spectroscopy for the determination of distillation property of kerosene. Vibrational Spectroscopy, 20(1999) 155-163.

19. Liu, R., R.L. Frost, and W.N. Martens, Near infrared and mid infrared investigations of adsorbed phenol on HDTMAB organoclays. Materials Chemistry and Physics, 113(2009) 707-713.

20. Frost, R.L., H.J. Spratt, and S.J. Palmer, Infrared and near-infrared spectroscopic study of synthetic hydrotalcites with variable divalent/trivalent cationic ratios. Spectrochimica Acta Part A: Molecular and Biomolecular Spectroscopy, 72(2009) 984-988.

21. Ping Zhang，Guangren Qian, H.S., Xiuxiu Ruan, Jing Yang, Ray L. Frost. Mechanism of interaction of hydrocalumites (Ca/Al-LDH) with methyl orange and

348 acidic scarlet GR. Journal of Colloid and Interface Science, 365 (2012) 7-15.
349 22. Yan, Y., et al., Single-step synthesis of layered double hydroxides ultrathin
350 nanosheets. Journal of Colloid and Interface Science, 371 (2012) 15-19.
351 23. Guo, Y., et al., Adsorption of Arsenate on Cu/Mg/Fe/La Layered Double
352 Hydroxide from Aqueous Solutions. Journal of Hazardous Materials, 16 (2012)
353 142-149.
354 24. Ping Zhang, G.Q., Hongfei Cheng , Jing Yang , Huisheng Shi , Ray L. Frost,
355 Near-infrared and mid-infrared investigations of Na-dodecylbenzenesulfate
356 intercalated into hydrocalumite chloride (CaAl-LDH-Cl). Spectrochimica Acta Part A:
357 Molecular and Biomolecular Spectroscopy, 79 (2011) 548-553.
358 25. Morgan, D.L., et al., Determination of a Morphological Phase Diagram of
359 Titania/Titanate Nanostructures from Alkaline Hydrothermal Treatment of Degussa
360 P25. Chemistry of Materials, 20 (2008) 3800-3802.
361 26. Liu, C., et al., Synthesis and characterization of 5-fluorocytosine intercalated
362 Zn-Al layered double hydroxide. Journal of Solid State Chemistry, 181 (2008)
363 1792-1797.
364 27. Kristof, J., et al., Separation of Adsorbed and Intercalated Hydrazine in
365 Hydrazine-Hydrate Intercalated Kaolinite by Controlled-Rate Thermal Analysis.
366 Langmuir, 18 (2002) 1244-1249.
367

368 Table.1 Summary of MIR wavenumbers (cm^{-1}) and their assignment for C_3A and

369 CaAl-SDBS-LDH

Wavenumbers		
C_3A	CaAl-SDBS-LDH	Assignment
1625, 1543, 1484	1665	Water bending modes
	1425	Carbonate antisymmetric stretch
	1465, 1417	C–C aromatic stretch
	1176	S=O asymmetric stretch
	1216, 1040	S O symmetric stretch and anti-symmetric stretch
	1134, 1015	C–H aromatic in-plane bending
792, 593, 534	692, 560, 534	M–O lattice vibrations

370

371

372

373

374

375

376 Table.2 Summary of NIR wavenumbers (cm^{-1}) and their assignment for C_3A and

377 CaAl-SDBS-LDH

Wavenumbers		
C_3A	CaAl-SDBS-LDH	Assignment
	8300	C-H overtone stretching vibrations
	7193, 7093, 6907, 6859	OH stretching vibrations
	5870, 5815, 5776	The overtones of C–H stretching vibrational modes
	5233, 5164, 5075	water OH vibrations
	4644, 4609, 4330, 4393, 4260, 4180	$(CO_3)^{2-}$ and CH groups

List of Tables

Table.1 Summary of MIR wavenumbers (cm^{-1}) and their assignment for C_3A and CaAl-SDBS-LDH

Table.2 Summary of NIR wavenumbers (cm^{-1}) and their assignment for C_3A and CaAl-SDBS-LDH

Fig. 1.XRD patterns of samples of C_3A and CaAl-SDBS-LDH scanned from 2° to 10° (a) and 10° to 65° (b).

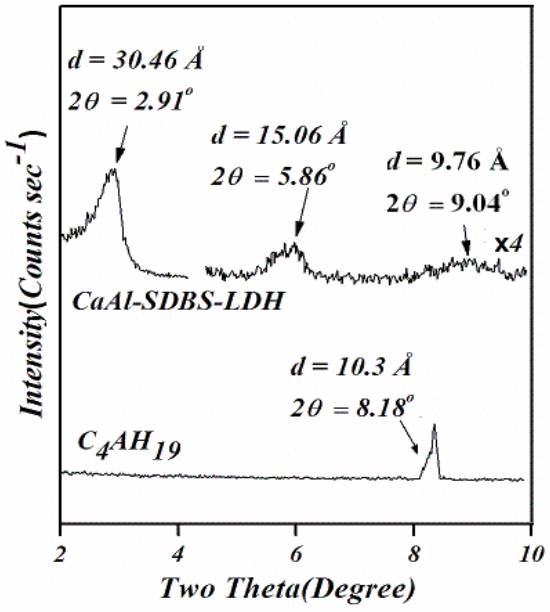

(a)

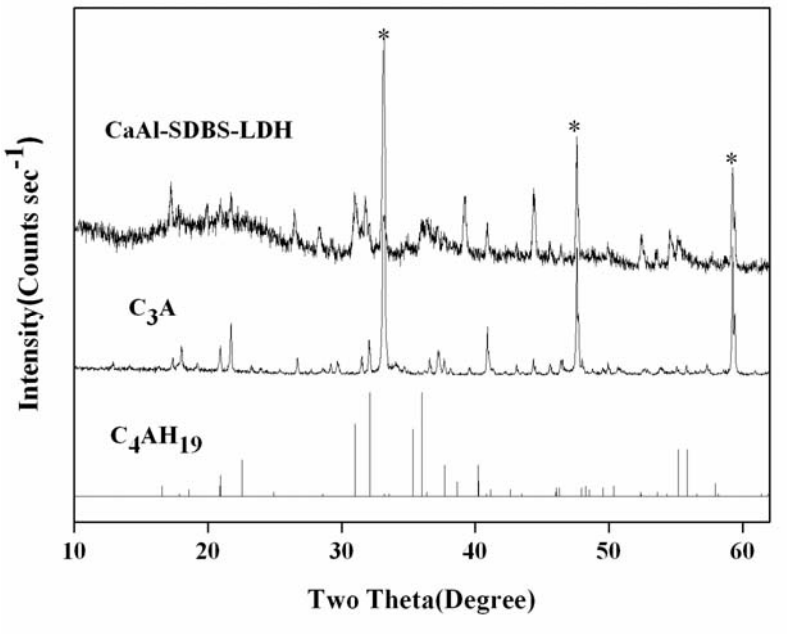

(b)

Fig.2 The 4000-500 cm^{-1} region of IR spectra of samples of C_3A and CaAl-SDBS-LDH

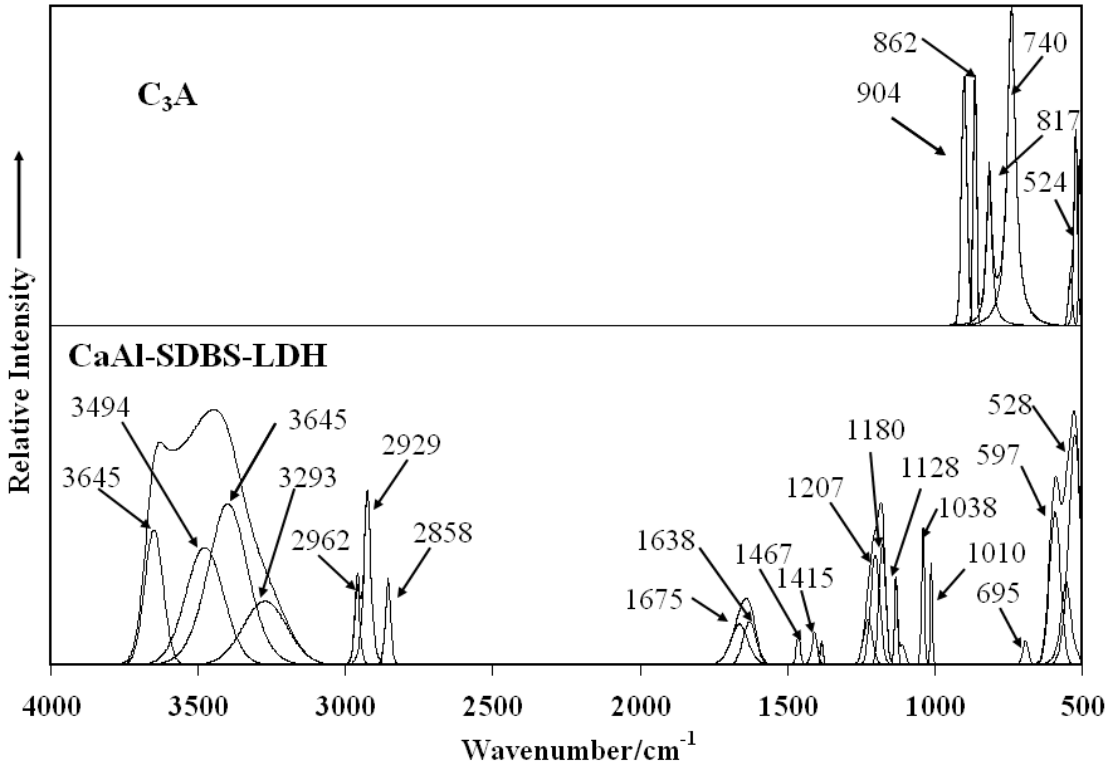

Fig.3 The 9000-4000 cm^{-1} region of NIR spectra of samples of CaAl-SDBS-LDH

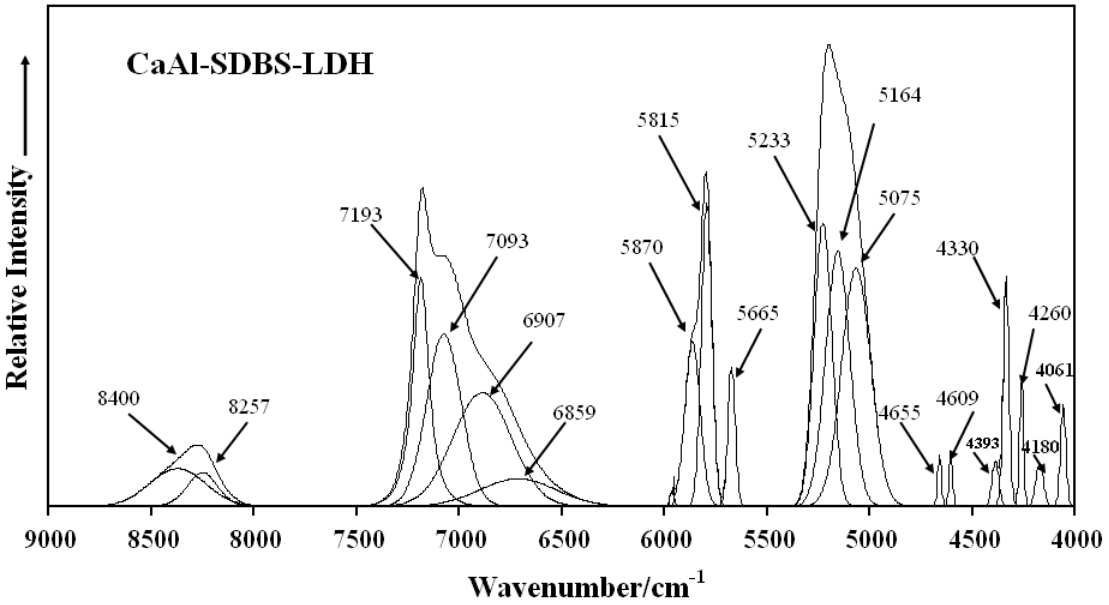

Fig.4 The TG and DTA curves of C_3A (a); CaAl-SDBS-LDH (b)

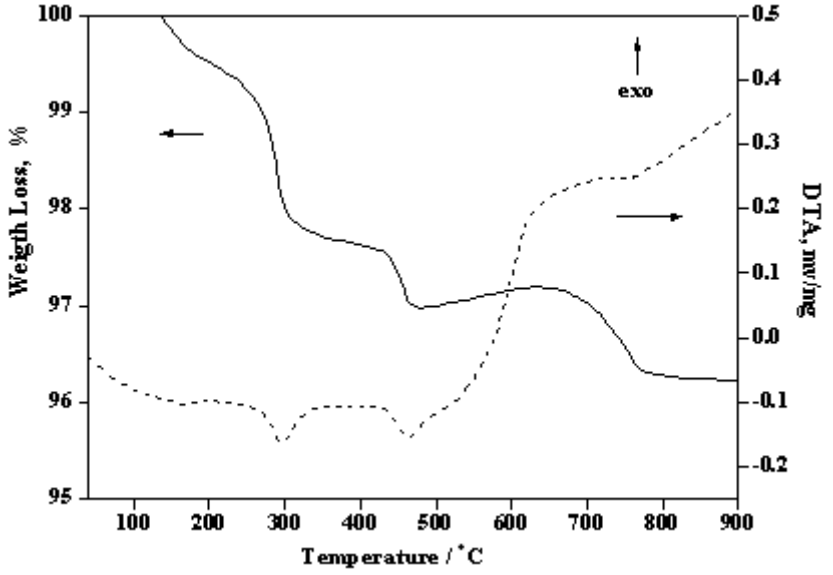

(a)

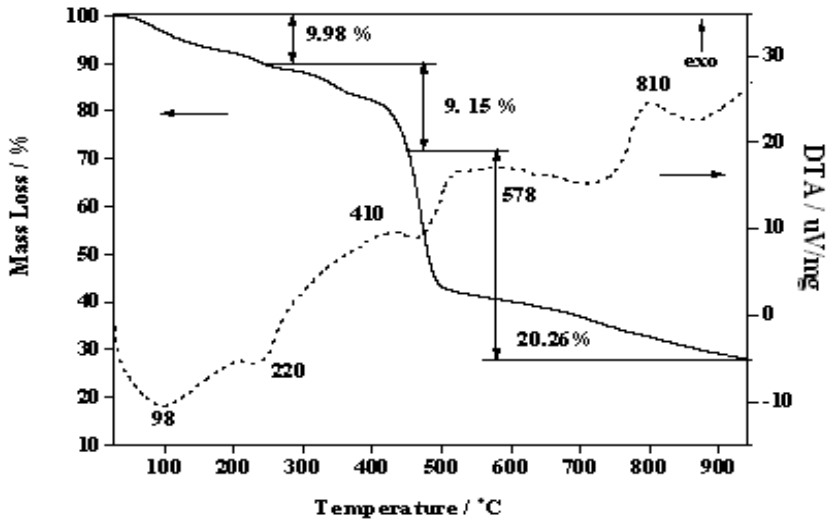

(b)

Fig.5 The SEM micrographs of C_3A(a); CaAl-SDBS-LDH (b)

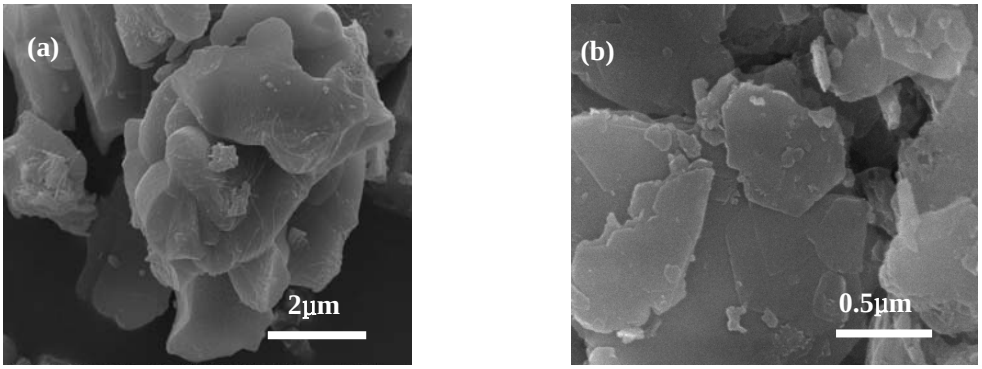

List of Figures